Organically bound tritium (OBT) and carbon-14 accumulation in the sediments off the mouth of the Rhône river

Philippe Jean-Baptiste, M. Fontugne, E. Fourré, S. Charmasson, L. Marang, F. Siclet

Organically Bound Tritium (OBT) and Carbon-14 accumulation in the sediments off the mouth of the Rhône river

P. Jean-Baptiste[1], M. Fontugne[1], E. Fourré[1], S. Charmasson[2], L. Marang[3], F. Siclet[3]

[1]*CEA-CNRS-UVSQ, Laboratoire des Sciences du Climat et de l'Environnement, Centre de Saclay, 91191, Gif-sur-Yvette, France*

[2]*IRSN, PSE-ENV/SRTE, Laboratoire de Recherche sur les Transferts des radionucléides au sein des écosystèmes Aquatiques (LRTA), Centre IFREMER, 83507 La Seyne-sur-Mer, France.*

[3]*EDF-R&D, Laboratoire National Hydraulique et Environnement, 6 Quai Wattier, 78401 Chatou, France*

Corresponding author: Philippe Jean-Baptiste (pjb@lsce.ipsl.fr)

Abstract

We have studied the recent history of Organically Bound Tritium (OBT) and carbon-14 in suspended organic matter carried by the Rhône from the analysis of two cores collected in the sedimentary cone off the river mouth. Measured OBT and carbon-14 concentrations highlight characteristic anthropogenic traces in the suspended matter of the Rhône, with a peak of tritium and carbon-14 commencing at the start of the 1970's and extending over some thirty years. In spite of the influence of the atmospheric nuclear tests of the 1950's and 1960's and of the discharges of carbon-14 by the nuclear industries located along the Rhône, carbon-14 levels are

low due to the diluting effect of a refractory carbon component very low in carbon-14 present in the coastal sediments. Organically bound tritium (OBT) levels are well above the modern background created by the global imprint of bomb-tritium. Detailed study of the impact of the various contribution to the tritium peak indicates that these traces are mostly the result of the sediments in the Rhône being contaminated by past tritium releases by the watchmaking industry in the upper Rhône.

Keywords: Rhône prodelta; tritium; carbon-14; radioactive contamination; watchmaking industry

1. Introduction

The Rhône valley and the french nuclear-based industry share a long common history that started in the 1950s and 1960s with the commissioning of several major nuclear facilities dedicated to the production and reprocessing of plutonium and tritium. Today, the Rhône valley has the highest density of nuclear activities in Europe (Fig. 1), comprising two major nuclear sites (Marcoule and Tricastin) housing civilian and military activities and four nuclear power plants (Bugey, Saint-Alban, Cruas, Tricastin) with a total of 14 reactors (to which Crey-Malville should be added; this reactor was decommissioned in 1997). Over this period, a repository of artificial radionuclides has built up in the sediments delivered to the Mediterranean Sea and deposited in the sedimentary prism (Rhône prodelta) off the mouth of Rhône river. These sediments enable us to reconstruct the history of the inputs to the river of some radionuclides, including ^{60}Co, ^{137}Cs, ^{238}Pu, $^{239,240}Pu$ (Charmasson et al., 1998; Charmasson, 2003 ; Lansard et al., 2007). This paper presents a study of the vertical distribution of organically bound tritium (OBT) and carbon-14 in two sediment cores taken from the Rhone prodelta. The aim of the study was to obtain the first historical record of these two radionuclides in the suspended matter of the Rhône and to evaluate the extent of anthropogenic tritium and carbon-14 accumulation in the Rhône prodelta. Throughout the text, tritium levels are expressed in Tritium Units (TU), 1 TU corresponding to a T/H ratio of 10^{-18}. The unit used for carbon-14 is the pmC (% modern Carbon): with this unit, the pre-industrial specific activity for carbon-14 (226 Bq/kgC) corresponds to 100 pmC (Mook and van der Plicht, 1999).

2. Background

The Rhône (812 km long) is one of the main rivers in Europe. It rises in the Swiss Alps at an altitude of 2,200 m and ends in the Camargue delta before flowing into the Gulf of Lyon, a large continental shelf located in the northwestern Mediterranean Sea. It is the largest river flowing into the western Mediterranean basin, both in terms of water and particulate matter, accounting for 80% of the solid riverine inputs to the Gulf of Lions (Monaco et al., 1990). At the mouth of the Rhône the particulate matter settles quickly and creates a sedimentary prism. Its proximal fan, as the extension to the Rhône's land-based channel, is marked by a slight slope. The prodelta itself starts with a clean break to the slope and extends to a depth of 60 m. It is characterised by the highest rates of sedimentation in the Gulf of Lion, reaching up to between 0.2 and 0.5 m yr^{-1} (Charmasson et al., 1998). The distal fan, below a depth of 60 m, corresponds to a second break in the slope and is characterised by less energetic hydrodynamics that favour finer particles settling with sedimentation rates no greater than a few millimetres per year (Radakovitch et al., 1999). This sedimentary complex captures a large proportion of the pollutants carried by the Rhône.

3. Origin of carbon-14 and tritium in the organic matter of Rhône sediments

The origin of the particulate organic matter in the Rhône is 90% non-native (allochthonous), in other words due to the leaching of the catchment areas (Lansard et al., 2009 ; Hamelin-Vivien et al., 2010). The remaining 10% corresponds to the autochtonous organic matter, that is the organic matter photosynthesised by plants in the river itself. As a consequence, the carbon-14 and tritium tagging of organic suspended matter in the Rhône has two origins: the export of organic residues from

87 catchment areas, influenced by the tritium (HTO) and carbon-14 atmospheric
88 contents, and organic matter formed in-situ, influenced by the tritium and carbon-14
89 content of the Rhône waters.

90 3.1. Natural sources

91 Tritium (^{3}H) and carbon-14 (^{14}C) are produced naturally in the atmosphere by the
92 effect of cosmic radiation principally on nitrogen. Tritium enters into the water cycle in
93 the form of a molecule of tritiated water (HTO), then spreads into the biosphere as
94 Tissus Free Water Tritium (TFWT) and organically bound tritium (OBT) - Eyrolle et
95 al., (2018). The natural T/H ratio for surface waters is in the range 10^{-18} - 10^{-17}, i.e. 1
96 to 10 TU (Cauquoin et al., 2015). In the same way, carbon-14 is oxidised to form a
97 molecule of carbon dioxide ($^{14}CO_2$) that enters the natural cycle of organic carbon
98 (photosynthesis) and inorganic carbon.
99
100 3.2. Global human-made inputs

101 Substantial amounts of tritium and carbon-14 were released into the environment
102 by the atmospheric nuclear tests of the 1950's and 1960's. When the test ban treaty
103 came into force in 1963, the atmospheric content of carbon-14 had reached 200
104 pmC, i.e. twice the natural level (Nydal and Lövseth, 1996) and that of tritium 2,000
105 TU in the northern hemisphere (IAEA water isotopes database at
106 https://nucleus.iaea.org /wiser/gnip.php). Because carbon and hydrogen in the
107 biosphere equilibrates isotopically with the atmosphere, this global tritium and
108 carbon-14 imprint of the atmospheric nuclear tests is recorded in vegetation, and
109 therefore, in the organic matter deposited in particulate form in the Rhône and along
110 the Mediterranean coast, associated with the leaching of organic material in the soil.

111

112 3.3. Tritium and carbon-14 of local industrial origin

113 3.3.1 Local gaseous discharges of carbon-14 and tritium (HTO)

114 Atmospheric discharges of tritium (HTO) influencing the Rhône catchment are
115 mainly due to the nuclear activities of the Marcoule site, operated by the French
116 Atomic Energy Commission (CEA) and the AREVA company, and of the CEA-Valduc
117 military site (Fig. 2); gaseous tritium discharges from the nuclear power stations
118 currently make up less than 1% of the total (and hence even less in the past). These
119 atmospheric discharges of tritium produce substantial local traces in the land
120 environment. The data available for the Marcoule site indicates levels of tritium (OBT)
121 in the organic matter of plants up to 20,000 TU for the most exposed zones
122 (Rousset-Debet, 2012). Measurements taken for lichens in Valduc (Daillant et al.,
123 2001) indicate maximum values on the order of 80,000 TU for the most exposed
124 lichens. Since the origin of the particulate organic matter in the Rhône is 90% non-
125 native (allochthonous), in other words due to the leaching of the catchment areas
126 (Lansard et al., 2009 ; Hamelin-Vivien et al., 2010), the leaching of tritiated organic
127 material in soil may therefore have a significant effect on organic tritium in suspended
128 matter and sediments.

129 With respect to airborne discharges of carbon-14, only recent data are available,
130 because previously carbon-14 releases were not recorded separately from other
131 beta/gamma emitters. Anyway, the traces in the land environment due to discharges
132 into the atmosphere of carbon-14 are low due to a net predominance (80%) of
133 discharges in the form of methane (Le Guen and Siclet, 2009) that cannot be
134 absorbed by vegetation. Nevertheless, a slight increase is noted in the local land
135 vegetation on the order of 5% to 15% (Roussel-Debet, 2012).

136

137 3.3.2 Direct liquid discharges of carbon-14 and tritium (HTO) into the Rhône

138 The two major contributors to liquid discharges of tritium (in the form of HTO) into
139 the Rhône river are the Marcoule nuclear site and the nuclear power plants (Jean-
140 Baptiste et al., 2018). In the past, Marcoule releases were predominant, but today
141 releases are mainly due to the nuclear power plants (Fig. 3). Unfortunately, as noted
142 above for carbon-14 airborne discharges, only recent data for liquid discharges of
143 carbon-14 are available, because previously carbon-14 releases were not recorded
144 separately from other beta/gamma emitters.

145

146 3.3.3 Indirect liquid discharges of tritium (HTO) into the Rhône

147 CEA-Valduc is located in Bourgogne to the north-east of Dijon. The local
148 hydrology connects it to the Rhône via the Tille and the Saône. Although its tritium
149 discharges are in gaseous form only (mostly HTO), when a large amount of tritium (in
150 the form of HTO) are released into the atmosphere, it produces significant local
151 traces in the river network (Guétat et al., 2013). In the absence of dedicated studies,
152 the extent of the tritium contamination of the rivers around Marcoule and Valduc are
153 not known precisely. For several decades CEA-Valduc was the largest emitter of
154 tritium in the atmosphere in France. Based on the data of Guétat et al. (2013), the
155 proportion of tritium from gaseous discharges carried away by the local river network
156 can be estimated at around 2% (Jean-Baptiste et al., 2018). Here, we assume that
157 this figure also applies to Marcoule.

158

159 3.3.4 Tritium (OBT) discharges into the upper Rhône from the watchmaking industry

160 Substantial quantities of tritium (as a substitute for radium) were used between
161 1960 and 1990 by the watchmaking industry (Krejci and Zeller, 1979). Several
162 production units for fluorescent paints based on tritiated polystyrene supplied
163 numerous watchmaking workshops, principally in Switzerland but also, to a lesser
164 extent, in eastern France. This use of tritiated organic material is linked with the
165 significant traces found in sediments and suspended matter of the Rhône (Gontier
166 and Siclet, 2011; Jean-Baptiste et al., 2018), although we cannot say if these are due
167 to past direct deposits into the Rhône or indirect deposits via the catchment areas.
168 These traces are at their highest in the upper Rhône, upstream of Creys Malville, the
169 northernmost nuclear power station on the Rhône, with current values in sediments
170 between 10^5 - 10^6 TU (Jean-Baptiste et al., 2007) but are observed all along the river
171 (Fig. 4). This situation is only found in the Rhône - no such tritium contamination of
172 the sediments is observed for the other major French rivers where nuclear power
173 stations are also in operation (Gontier and Siclet, 2011).
174
175 **4. Methods**
176
177 KBROUS and KB-06 cores were analysed to determine the amounts of tritium
178 (OBT) and carbon-14 in the sedimentary organic matter. The sediment cores were
179 taken with a Kullenberg corer in November 2001 during the REMORA 2 campaign of
180 the French Institute of Radioprotection and Nuclear Safety (IRSN). The KBROUS
181 core was extracted close to the mouth of the Rhône (43°18.30'N, 4°51.01'E) where
182 the sedimentation rates are the highest, thus ensuring a good temporal resolution,
183 while KB-06 (43°18.02'N, 4°52.62'E) was taken further offshore (Fig. 1 inset). The
184 cores were kept in cold storage and then cut into 10 cm sections. The sediment

185 samples were then lyophilised during 48 hours to ensure a complete removal of the
186 water, passed through a 2 mm sieve, ground up, then packaged in sealed plastic
187 bags.

188 The amount of tritium was determined by mass spectrometry using the ^{3}He
189 regrowth method (Clarke et al., 1976), with a detection limit below 0.1 TU. The dried
190 sediment powder (typically 150 g) was transferred into a 100 mL low helium
191 diffusivity Corning 1724 glass bulb. To minimise ^{3}He blank, the bulbs were previously
192 baked in a flow of argon at 600°C for 24 hours to remove the helium dissolved in the
193 glass. All manipulations were undertaken in a glove-box flushed with argon to
194 minimize contamination by ambient air moisture. The bulbs were attached to a high
195 vacuum line and evacuated down to $<10^{-5}$ Torr, they were then flame-sealed. After
196 sealing, the samples were stored at -20°C to further minimise helium diffusion
197 through glass (Jean-Baptiste et al., 1989). After a period of storage of typically 100-
198 150 days, the bulbs were connected to the inlet line of a mass spectrometer for ^{3}He
199 analysis. The instrument is a MAP 215-50 noble gas mass spectrometer equipped
200 with a stainless steel low blank inlet system (^{3}He blank$< 3x10^{-20}$ mol). The analysis
201 protocol is described in detail by Jean-Baptiste et al. (2010).

202 The carbon-14 activities were measured by Accelerator Mass Spectrometry
203 (AMS) at the LMC14-ARTEMIS facility (Saclay). The sediment samples were de-
204 carbonated (HCl 0.5N) and rinsed with de-ionised water before being dried at 60°C in
205 a drying oven at the Laboratoire des Sciences du Climat et de l'Environnement
206 (LSCE). The samples were then introduced into quartz tubes in the presence of 500
207 mg of copper oxide and a silver thread. They were then heated to 835°C for 6 hours
208 in order to transform the organic material into CO_2 (Hatté et al., 2003).

209 Accuracies on tritium and carbon-14 measurements are given in the tables of
210 results.
211 In addition, following Gauthier and Hatté (2008), a few milligrams of sediment
212 were used to measure the stable organic carbon isotope composition ($\delta^{13}C$). The
213 measurements were carried out by EA-IRMS in continuous flow coupling an
214 elementary analyser (Fisons Instrument NA 1500 Element Analyser) to a mass
215 spectrometer (Thermo-Finigan Delta + XP Isotope-Ratio Mass Spectrometer). The
216 $\delta^{13}C$ is expressed in ‰ with respect to the standard PDB (Pee Dee Belemnite), with
217 precision of ±0.08 ‰.
218
219 **5. Results**
220
221 5.1 OBT and carbon-14 vertical profiles
222 The vertical profiles of organically bound tritium (OBT) and carbon-14 are shown
223 in Fig. 5 (see also Table 1 and 2). From the base to the top, the vertical profile of
224 OBT in the KBROUS core displays an increase up to an initial peak at 390 cm depth,
225 followed by two other peaks at 280 and 240 cm. The upper part of the core (230 cm
226 to 0 cm) shows a decrease in tritium content. A peak of OBT is also present in the
227 KB-06 core, with a maximum much nearer to the surface (30 - 40 cm deep) due to
228 the lower sedimentation rate in this area.
229 The vertical profiles of carbon-14 present similar variations but the difference
230 between the peaks and the baseline is much lower than for tritium. The carbon-14
231 activities are low (the majority are lower than 100 pmC) due to the diluting effect of
232 an ancient refractory carbon component very low in carbon-14 (~ 0 pmC) present in

233 the coastal sediments held in suspension (Cathalot et al., 2013). Taking 100 pmC as
234 a reference for pre-industrial carbon-14, the baseline values for KB-06 (37 pmC)
235 correspond to 37%-63% mixture of modern organic matter and ancient refractory
236 carbon. Using this mixing ratio, the peak value of 79.98 pmC recorded in the KB-06
237 core corresponds to a modern organic matter maximum of 216 pmC. This value is
238 close to the carbon-14 bomb-peak value of 200 pmC (Nydal and Lövseth, 1996).
239 Hence it does appear that a significant contribution from the carbon-14 bomb-peak
240 may have been captured in this sedimentary record.

241 $\delta^{13}C$ of organic carbon is reported in Tables 1 and 2. Values range between -
242 25.11‰ and -26.70‰ for KB-06 and between -25.11‰ and -27.31‰ for KBROUS.
243 $\delta^{13}C$ values within KB-06 are slightly greater than those of KBROUS, consistent with
244 the location of the core where there is more influence of marine conditions (see
245 below). The two cores display, from the base to the top, a similar and regular
246 decrease in the carbon isotopic composition, in good agreement with observations
247 for recent sediments and soils (Bentaleb and Fontugne, 1996): this 1‰ – 1.5‰
248 decrease in $\delta^{13}C$ values has to be related to the Suess effect and the atmospheric
249 input of CO_2 with a low $^{13}C/^{12}C$ ratio resulting from the combustion of fossil fuel since
250 the beginning of the industrial period (Friedly et al., 1986; Trundiger et al., 1999).

251 The cores received organic carbon from two sources: terrestrial suspended
252 matter from the Rhône and marine phytoplankton from the Mediterranean. In most
253 sedimentary environment marine planktonic organic carbon is isotopically heavier
254 than that of the carbon delivered to the ocean from terrestrial environments. Solution
255 of the mixing equation $\delta^{13}C = F_t \times \delta^{13}C_t + F_m \times \delta^{13}C_m$ (with $F_m + F_t = 1$) provides a
256 simple method for estimating the proportions of the two types of organic matter
257 present in a given sample (Calder and Parker, 1968; Fontugne and Duplessy, 1986;

Fontugne and Jouanneau, 1987). In this equation, F_t and F_m are the fractions of terrestrial and marine organic matter, and $\delta^{13}C_t$ and $\delta^{13}C_m$ are the isotopic composition of the terrestrial and marine organic carbon sources, respectively. Following Fontugne and Calvert (1992) and Fontugne et al. (1989), we use $\delta^{13}C$ values of -21‰ and -27‰ for the marine and terrestrial end-members, respectively. The calculation shows that the terrestrial fraction varies between 75% and 85% for KB-06 and between 85% and 90% for KBROUS.

5.2 Core timelines

The discharge of solid matter from the Rhône to the sea is characterised by large seasonal and interannual variations ; overall, on the order of 2 to 8 million tons per year ($Mt.yr^{-1}$), but it can reach up to 26.5 $Mt.yr^{-1}$ (Pont et al., 2002). The high discharge episodes, responsible for about 80% of the total amount delivered to the coast (Antonelli et al., 2004; Roussiez et al., 2005), occur during floods. Due to the impulsive nature of the discharge of solid matter, but also to the resuspension of surface sediments by storms (Aloisi et al., 1982), the core samples do not reflect a continuous sedimentation process. In addition, other processes such as bioturbation and biological uptake add further complexity to the establisment of a reliable chronology. Therefore, it is beyond the scope of the present study to produce a detailed chronology on which conclusions could be based. Nevertheless, it is very important to place the measured vertical profiles on a time scale to calculate decay-corrected OBT concentrations in each core and thus to obtain OBT levels at the time of deposition. In the following, we use the $^{239,240}Pu$ and ^{241}Am concentration measurements in the cores along with historical discharges of $^{239,240}Pu$ by the Marcoule site to infer a simplified chronology for each core assuming an average

sedimentation rate, as proposed by Lansard (2004). The main interest of these radionuclides is that, apart from the small imprint by the bomb-tests fallouts, they have a unique source in the Rhône river (the Marcoule site); the start of the releases, in the mid-1970's, thus constitutes a convenient tie-point.

5.2.1 KBROUS core

The vertical distribution of $^{239,240}Pu$ in the KBROUS core is reported by Lansard et al., 2007. The primary source of plutonium measured in the sediments near the Rhône mouth originates from the liquid effluents released by the Marcoule reprocessing plant. The chronology of these discharges is available from Eyrolle et al., 2004. The visual comparison of the $^{239,240}Pu$ profile with the history of plutonium liquid discharges from the Marcoule site allows us to estimate a mean sedimentation rate of 0.186 $m.yr^{-1}$ (Fig. 6). This average sediment accumulation rate is in good agreement with that determined by Lansard (2004) who concludes, based on the historical release of $^{239,240}Pu$ from Marcoule, that the average sedimentation rate for KBROUS over the last forty years is of the order of 0.17 m.yr-1

5.2.2 KB-06 core

In the KB-06 core the vertical distribution of ^{241}Am, an other artificial radionuclide released along with plutonium by Marcoule military activities, was measured by IRSN (unpublished results). The history of ^{241}Am discharges from the Marcoule site can be reconstructed from that of $^{239,240}Pu$ (Eyrolle et al., 2004) using the good correlation between $^{239,240}Pu$ and ^{241}Am observed in the KBROUS core (Fig. 7) and assuming that, since both radionuclides have the same strong affinity for solid particles, the

307 $^{241}Am/^{239,240}Pu$ ratio is not significantly modified between the liquid releases and the
308 deposition in the sediment. From the visual comparison of the ^{241}Am profile with the
309 history of ^{241}Am liquid discharges (Fig. 8), we deduce a mean sedimentation rate of
310 0.025 $m.yr^{-1}$.
311
312 5.3. Time-evolution of the OBT record

313 Figure 9 displays the time-evolution of the tritium (OBT) content of the organic
314 matter in the KB-06 and KBROUS cores. For each core, the time scale used is that
315 determined in Section 5.2. The tritium concentrations have been decay-corrected so
316 the OBT content is that of suspended organic matter at the date of deposition. In both
317 cores, tritium concentrations start to increase in the early 1970's and decrease after
318 1990. The chronological agreement between the two OBT profiles of Figure 9 shows
319 that our strategy of using average sedimentation rates gives coherent results in spite
320 of its oversimplification. For the KBROUS core (Fig. 9 black solid line), the higher
321 resolution relative to KB-06 allows us to distinguish two peaks, a first one reaching up
322 to 40,000 TU and a second one with values up to 30,000 TU. For 1986-1987, Gontier
323 et al. (1992) reported a tritium (OBT) value of 26,160 TU in surface sediments (0-3
324 cm) at the mouth of the Rhône. This is fully consistent with the tritium concentrations
325 recorded in the KBROUS core (see Fig. 9). Later on, tritium levels decrease strongly,
326 in agreement with tritium (OBT) measured in suspended matter at Arles in 2010-2011
327 (Jean-Baptiste et al., 2018).

328 The tritium maximum measured in the KB-06 core, 20,000 TU (black dotted line
329 Fig. 9), is lower than that of the KBROUS core. This decrease in tritium as distance
330 from the mouth increases, has already been noted by Gontier et al. (1992). It can be
331 explained by the fact that the size distribution of river suspended matter is shifted

towards larger particles compared to marine suspended matter (Eisma et al., 1991 ; Reynolds et al., 2010). Because of this, river particles tend to settle preferentially close to the river mouth. Therefore, sediments closer to the river mouth are proportionally richer in organic matter of riverine origin (i.e., with a greater tritium content) than sediments further offshore.

6. Attributing OBT levels in organic matter to the various known sources

6.1 Tritium from atmospheric nuclear tests

The OBT for the land-based organic material due to atmospheric nuclear tests is of the same magnitude as that for rain. The mean annual tritium content for rain peaks towards 2,000 TU in 1963 at the latitude of France. This figure is far lower than the maximum values recorded for the KBROUS core (~ 40,000 TU). This clearly indicates that atmospheric nuclear tests are not the main cause of the peak in tritium recorded in the Rhône prodelta.

6.2 Liquid tritium discharges

The OBT content of the organic matter at the surface of the KBROUS core (corresponding to year 2001) was 1855 ± 200 TU for a total annual liquid discharge of 200.8 TBq (Fig. 3). With the mean flow rate of the Rhône being 1700 $m^3 s^{-1}$, this discharge corresponds to an elevation of the tritium content of the river water of 31.4 TU. In comparison, on the Loire river (mean flow rate = 850 $m^3 s^{-1}$), where four nuclear electricity production sites are in operation with total annual liquid tritium discharges of about 150 TBq (EDF, 2007), the OBT level in sediments downstream of the nuclear plants in 2003 was only 55 TU (Gontier and Siclet, 2011), in spite of a

356 higher mean elevation of the tritium content of the river water (47 TU). The maximum
357 of the liquid discharge of tritium (HTO) to the Rhône reaches ~1000 TBq (Fig. 3),
358 corresponding to an additional tritium content of the river waters of 156 TU. Scaled to
359 the Loire river data, a tritium level in the organic matter on the order of 183 TU should
360 be expected. This value is far from the maximum values (40,000 TU) recorded in the
361 KBROUS core. These comparisons with the Loire river data clearly indicate that the
362 liquid tritium discharges cannot be held responsible for the high values of tritium
363 recorded in the Rhône prodelta. This fact is corroborated by the close examination of
364 the data which reveals that, whereas the tritium discharges start to increase again
365 after 1998 (with an increase by 70% between 1998 and 2010 – Fig. 3), the tritium
366 content of sediments decreases continuously (Fig. 9), thus indicating that the two
367 records are not correlated.
368
369 6.3 Gaseous tritium discharges
370 We have seen (Section 3.3.1) that gaseous tritium (HTO) discharged into the
371 atmosphere later appears in the land-based environment. The two largest emitters of
372 tritium into the atmosphere are the CEA-Valduc and Marcoule sites. Environmental
373 data gathered around these sites (Section 3.3.1) show that these releases have a
374 very significant effect on the local land vegetation. However, the global influence at
375 the scale of the Rhône watershed, and therefore on the organic matter transferred to
376 the river, remains to be quantified. In the study into the influence of tritium gaseous
377 discharges on the environment around the Bruyère-le-Châtel nuclear site operated
378 by CEA, Baglan et al. (2011) demonstrated that the tritium content in the land-based
379 organic material decreases with distance following an exponential rule described by
380 the formula:

$$(T/H) = (T/H)^0 + (T/H)^{max} \exp(-r/r_0) \quad (1)$$

where r is the distance, $(T/H)^{max}$ is the value in the immediate environment of the source of the discharge (corresponding to r=0) and $(T/H)^0$ is the value from background noise. Baglan et al. (2011) suggest a value for r_0 equal to 0.8 km. Applied to the data obtained around Marcoule in 2008-2011 by Roussel-Debet (2012), it is noted that this value is satisfactory for the local environment, but minimises the influence of discharges beyond a few kilometres (Fig. 10). The data for Marcoule is better described using a linear combination of two exponentials, one as near-field with an r_0 of 0.8 km and a second with an r'_0 equal to 8 km which increases the distance influenced by the discharge to 60-80 km:

$$(T/H) = (T/H)^0 + (T/H)^{max} [\exp(-r/r_0) + 0.1 \exp(-r/r'_0)] \quad (2)$$

with $(T/H)^{max}$ = 30,000 TU. Over the same period 2008-2011, the mean value for gaseous tritium discharge from Marcoule was D^T= 302 TBq.yr^{-1}.

The mean value for year n of the tritium added to the land vegetation by the gaseous tritium releases D^T_n can therefore be written :

$$(T/H)_n = A^{-1} (T/H)_n^{max} \int_0^{\infty} [\exp(-r/r_0)+0.1 \exp(-r/r'_0)] 2\pi r \, dr \quad (3)$$

where A is the total surface area of the Rhône watershed (A ~100000 km^2). Since formula (3) implies that $(T/H)_n^{max}$ is proportional to the annual discharge D^T_n, $(T/H)_n^{max}$ can be expressed as $(T/H)_n^{max} = \alpha D^T_n$, with α= 30,000/302 by reference to the situation around Marcoule in 2008-2011.

Solving the integral in formula (3) leads to :

$$(T/H)_n = 2\pi A^{-1} \alpha D^T_n \times [r_0^2 + 0.1 r'^2_0] \quad (4)$$

403 Finally, the mean tritium content of land vegetation for the whole Rhône
404 catchment under the influence of the gaseous discharges from both Marcoule and
405 Valduc for the year n can be expressed as :

406 $$(T/H)_n^{total} = (T/H)^0_n + (T/H)_n^{Marcoule} + (T/H)_n^{Valduc} \quad (5)$$

407 The peak value for the tritium gaseous discharges by Marcoule and Valduc
408 occurred around 1974 with 8600 TBq and 38800 Tbq respectively (Fig. 2). This
409 corresponds to $(T/H)_{1974}^{Marcoule}$ = 378 TU and $(T/H)_{1974}^{Valduc}$ = 1704 TU. Taking
410 $(T/H)^0_{1974}$ = 100 TU (IAEA database at https://nucleus.iaea.org /wiser/gnip.php), the
411 mean tritium content for the land vegetation of the whole Rhône catchment under the
412 influence of the discharges of Marcoule and Valduc at their historical peak of 1974
413 amounts to 2182 TU. This value represents about 5% of the tritium peak value
414 recorded in the KBROUS core. Moreover, this estimate is probably an upper limit for
415 the following reasons:

416 - The function describing the decreasing influence of the discharge with the
417 distance was deliberately chosen as an envelope curve.

418 - The integration over 360° is certainly an overestimation as the wind rose has a
419 very pronounced directional element: at the Marcoule site for example, the wind
420 (Mistral) blows from the north more than half of the time.

421 - A substantial proportion of the gaseous discharges from Valduc enters the River
422 Seine basin.

423 - The calculation does not take into account the smoothing effect caused by the
424 fact that the residence time of the organic matter in the land vegetation is greater
425 than one year.

426 This probable overestimation by formula (5) is consistent with the fact that, in the
427 case of Valduc, the comparison of the tritium contents of the sediments in the Rhône

428 downstream of Le Bugey power station and upstream of Saint Alban power station
429 (Gontier and Siclet, 2011) reveals no anomaly associated with the confluence of the
430 Saône (see Fig. 1). With regard to Marcoule, the tritium contents measured in the
431 sediments of the Rhône at the level of Tricastin power station (Gontier and Siclet,
432 2011) are similar to those measured in the prodelta. As Tricastin is to the north of the
433 Marcoule site and therefore little influenced by its discharges (Roussel-Debet, 2012),
434 this again suggests, as with the case of Valduc, that the imprint of gaseous
435 discharges from Marcoule in the sediments is masked by a much larger signal. This
436 inevitably points to the legacy of the past use of tritiated luminous paints by the
437 watchmaking industry in the upper Rhône area.

438 As already pointed out in Section 3.3.4, the tritium anomaly in the upstream
439 sediments of the Rhône, attributed to the watchmaking industry, is still very
440 pronounced, with maximum values in the range 10^5 to 10^6 TU between 2002-2005
441 near to the Swiss border (Jean-Baptiste et al., 2007). This shows that there is still a
442 considerable amount of tritium stored in the upstream Rhône sediments. This
443 quantity of stored sediment, whose tritium-contaminated particulate matter moves
444 from upstream to downstream particularly when the dams are flushed (every three
445 years from the 1970s until 2003), has a very high T/H ratio. Due to its scale, this
446 contamination of the Rhône sediments seems capable by itself of explaining what
447 lies behind the peak in tritium recorded in the prodelta sediments, masking all other
448 sources of tritium.

449

450 **7. Conclusion**

451 Tritium (OBT) and carbon-14 levels in suspended organic matter carried by the
452 Rhône over the period 1970-2001 were obtained based on the study of two sediment

453 cores collected in the sedimentary cone off the river mouth. The main conclusions of
454 the present work are as follows:
455 - Measured tritium and carbon-14 concentrations display a peak commencing at
456 the start of the 1970s and extending over some thirty years.
457 - The source of the carbon-14 peak is difficult to establish due to the fact that
458 carbon-14 releases by the nuclear industry are unknown (until recently, carbon-14
459 releases were not recorded separately from other beta/gamma emitters). However, it
460 appears that a significant contribution from the carbon-14 bomb-peak may have been
461 captured in the sedimentary record. Anyway, carbon-14 levels remain low (below the
462 modern carbon-14 natural value of 100 pmC) because of the diluting effect of a
463 refractory carbon component very low in carbon-14 present in the coastal sediments.
464 - Organically bound tritium levels are more pronounced, with maximum values up
465 to 40,000 TU (i.e., 20 times the tritium peak of the atmospheric nuclear tests of the
466 1950's and early 1960's).
467 - Detailed study of the impact of the various contributions to the OBT seen in the
468 sedimentary record strongly suggests that these high tritium levels cannot be
469 explained neither by the bomb-peak nor by the releases of the nuclear industry but
470 are the result of the sediments in the Rhône being contaminated from upstream to
471 downstream by the past utilisation of tritiated luminous paints by the watchmaking
472 industry. This contamination is at its highest in the upper Rhône, upstream of Creys
473 Malville, the northernmost nuclear power station on the Rhône. Its influence, which is
474 well documented all along the river, masks all other sources of tritium and seems
475 capable by itself of explaining what lies behind the peak in tritium recorded in the
476 prodelta sediments.
477

478 **References**

479 Aloisi J.C., Cambon J.P., Carbonne J., Cauwet G., Millot C., Monaco A. and Pauc H.
480 (1982) Origin and role of the bottom nepheloid layer in the transfer of particles
481 into the marine environment. Application to the Gulf of Lions. Oceanologica Acta
482 5 (4), 481-491.

483 Antonelli C., Provansal M. and Vella C. (2004) Recent morphological channel
484 changes in a deltaic environment. The case of the Rhone River, France.
485 Geomorphology 57, 385–402.

486 Baglan, N., Alanic, G., Le Meignen, R., Pointurier, F. (2011) A follow-up of the
487 decrease of non-exchangeable organically bound tritium levels in the
488 surroundings of a nuclear research center. J. Environ. Radioact. 102, 695-702.

489 Bentaleb I., Fontugne M. (1996) Anthropogenic CO_2 invasion of the surface Ocean:
490 its influence on the organic carbon isotope composition of phytoplankton.
491 C.R.Acad. Sci., Paris, Ser. IIa, 322, 743-748.

492 Calder, J. A. and Parker, P. L. (1968) Stable carbon isotope ratio as indices of
493 petrochemical pollution of aquatic systems. Environ. Sci. Technol., 2 , 535-539.

494 Cathalot, C., Rabouille, C., Tisnérat-Laborde, N., Toussaint, F., Kerhervé, P.,
495 Buscail, R., Loftis, K., Sun, M.Y., Tronczynski, J., Azoury, S., Lansard, B.,
496 Treignier, C., Pastor, L., Tesi, T. (2013) The fate of river organic carbon in
497 coastal areas: A study in the Rhône river delta using multiple isotopic ($\delta^{13}C$,
498 $\Delta^{14}C$) and organic tracers. Geochimica et Cosmochimica Acta 118, 33-55.

499 Cauquoin, A., Jean-Baptiste, P., Risi, C., Fourré, E., Stenni, B., Landais, A. (2015)
500 The global distribution of natural tritium in precipitation simulated with an

501 Atmospheric General Circulation Model and comparison with observations. Earth
502 Planet. Sci. Lett. 427, 160-170.

503 Charmasson S. (2003) ^{137}Cs inventory in sediment near the Rhone mouth: role
504 played by different sources. Oceanologica Acta 26, 435–441.

505 Charmasson S., Bouisset P., Radakovitch O., Pruchon A.S., Arnaud M. (1998) Long-
506 core profiles of ^{137}Cs, ^{134}Cs, ^{60}Co and ^{210}Pb in sediment near the Rhone River
507 (Northwestern Mediterranean Sea). Estuaries 21, 367–378.

508 Clarke, W.B., Jenkins, W.J., Top, Z. (1976) Determination of tritium by mass
509 spectrometry measurement of $^{3}He^{+}$. Int. J. Appl. Radiat. Isot. 27, 515 - 522.

510 Daillant, O., Pigrée, G., Gueidan, C., Jacquiot, L. (2001) Recherche de tritium
511 organiquement lié dans les lichens des environs de Valduc. Rapport de
512 l'Observatoire Mycologique pour la Structure d'Echange et d'Information sur
513 Valduc (SEIVA), Observatoire Mycologique, F-71250 Mazille.

514 EDF (Electricité de France) (2007) Nucléaire & Environnement 2007 Report, 36pp.

515 Eisma, D., Bernard, P., Cadée, G.C., Ittekkott, V., Kalf, J., Laane, R., Martin, J.M.,
516 Mook, W.G., Van Put, A., Schuhmacher, T. (1991) Suspended-matter particle
517 size in some west-european estuaries : Part I : particle size distribution.
518 Netherlands Journal of Sea Res. 28, 193-214.

519 Eyrolle F., Charmasson S., Louvat D. (2004) Plutonium isotopes in the lower
520 reaches of the River Rhone over the period 1945–2000: fluxes towards the
521 Mediterranean Sea and sedimentary inventories. J. Environ. Radioact. 72, 273–
522 286.

523 Eyrolle-Boyer, F., Boyer, P., Claval, D., Charmasson, S. (2014) Apparent enrichment
524 of organically bound tritium in rivers explained by the heritage of our past. J.
525 Environ. Radioact. 136, 162-168.

526 Eyrolle, F., Ducros, L., Le Dizès, S., Beaugelin-Seiller, K., Charmasson, S., Boyer,
527 P., Cossonnet, C. (2018) An updated review on tritium in the environment. J.
528 Environ. Radioact. 181, 128-137.

529 Fontugne M. and Jouanneau J.M. (1987) Modulation of the particulate organic
530 carbon flux to the ocean by a macrotidal estuary: organic carbon isotopes
531 evidence from the Gironde system. Estuarine Coastal Shelf Sci. 24, 377-387.

532 Fontugne M., Paterne M., Calvert S.E., Murat A., Guichard F., Arnold M. (1989)
533 Adriatic deep warer formation during the Holocene. Implication for the re-
534 oxygenation of the deep eastern Mediterranean Sea. Paleoceanography 4, 199-
535 206.

536 Fontugne M. and Calvert S.E. (1992) Late Pleistocene variability of the carbon
537 isotopic composition of organic matter in the eastern Mediterranean: monitor of
538 changes in carbon sources and atmospheric CO_2 concentrations.
539 Paleoceanography 7, 1-20.

540 Friedly H., Lötscher H., Oeschger, H., Siegenthaler U., Stauffer, B. (1986) Ice core
541 record of the $^{13}C/^{12}C$ ratio of the atmospheric $C0_2$ in the two past centuries.
542 Nature 324, 237-238.

543 Gauthier C. and Hatté, C. (2008) Effects of handling, storage and chemical
544 treatments on ^{13}C values of continental sediments. Geochem. Geophys.
545 Geosyst., 9(8), Q08011, doi:10.1029/2008GC001967.

546 Gontier, G., Grenz, C., Calmet, D., Sacher, M. (1992) The contribution of Mytilus sp.
547 in radionuclide transfer between water comlumn and sediments in the estuarine
548 and delta systems of the Rhône River. Estuarine Coastal Shelf Sci. 34, 593-601.

549 Gontier, G. and Siclet, ,F. (2011) Organic tritium in freshwater ecosystems: long-term
550 trends in the environment of French nuclear power plants. Radioprotection 46,
551 457-491.

552 Guétat, P., Le Goff, P., Boyer, C., Duda, J.M. (2013) Apports de la surveillance du
553 centre CEA-Valduc sur la connaissance des transferts de l'eau tritiée
554 atmosphérique dans les différents compartiments de l'environnement.
555 Radioprotection 48, 367-389.

556 Harmelin-Vivien, M., Dierking, J., Banaru, D., Fontaine, M.F., Arlhac, D. (2010)
557 Seasonal variation in stable C and N isotope ratios of the Rhone River inputs to
558 the Mediterranean Sea (2004–2005). Biogeochemistry 100, 139-150.

559 Hatté, C., Poupeau, J.J., Tatman, J.F., Paterne, M. (2003) Development of an
560 automated system for preparation of organic samples. Radiocarbon 45, 421-430.

561 Jean-Baptiste, P., Andrié , C., Lelu, M. (1989) The diffusion of helium through glass.
562 Glass Technol. 30, 228–230.

563 Jean-Baptiste, P., Baumier, D., Fourré, E., Dapoigny, A., Clavel, B. (2007) The
564 distribution of tritium in the terrestrial and aquatic environments of the Creys-
565 Malville nuclear power plant (2002-2005). J. Environ. Radioact. 94, 107-118.

566 Jean-Baptiste, P., Fourré, E., Dapoigny, A., Baumier, D., Baglan, N., Alanic, G.
567 (2010) ^{3}He mass spectrometry for very low-level measurement of organic tritium
568 in environmental samples. J. Environ. Radioact. 101, 185-190.

569 Jean-Baptiste, P., Fontugne, M., Fourré, E., Marang, L., Antonelli, C., Charmasson,
570 S., Siclet, F. (2018) Tritium and radiocarbon levels in the Rhône river delta and
571 along the French Mediterranean coastline. J. Environ. Radioact. 187, 53-64.

572 Krejci, K. and Zeller, A. (1979) Tritium pollution in the Swiss luminous compound
573 industry. In: Behaviour of tritium in the Environment. IAEA Proceedings series
574 STI/PUB/498, 65-77.

575 Lansard B., Charmasson, S., Gascó, C., Antón, M.P., Grenz, C., Arnaud, M. (2007)
576 Spatial and temporal variations of plutonium isotopes (^{238}Pu and ^{239,240}Pu) in
577 sediments off the Rhone River mouth (NW Mediterranean). Sci. Total Environ.
578 376, 215–227.

579 Lansard, B. (2004) Distribution et remobilisation du Plutonium dans les sédiments du
580 prodelta du Rhône (Méditerranée Nord-Occidentale). PhD thesis, Université de la
581 Méditerranée Aix-Marseille II, pp.279.

582 Lansard, B., Rabouille, C., Denis, L., Grenz, C. (2009) Benthic remineralization at the
583 land-ocean interface: A case study of the Rhône River (NW Mediterranean Sea).
584 Estuarine Coastal Shelf Sci. 81, 544-554.

585 Le Guen, B., Siclet, F. (2009) Impact du carbone-14 autour des centrales nucléaires
586 EDF. Radioprotection 44, 495-504.

587 Monaco, A., Courp, T., Heussner, S., Carbonne, J., Fowler, S.W., Deniaux, B. (1990)
588 Seasonality and composition of particulate fluxes during ECOMARGE-I, western
589 Gulf of Lions. Cont. Shelf Res. 10, 959-987.

590 Mook, W.G. and van der Plicht, J. (1999) Reporting C-14 activities and
591 concentrations. Radiocarbon 41, 227-239.

592 Nydal, R. and Lövseth, K. (1996) Carbon-14 Measurements in Atmospheric CO_2 from
593 Northern and Southern Hemisphere Sites, 1962-1993. ORNL/CDIAC-93, NDP-
594 057. Carbon Dioxide Information Analysis Center, Oak Ridge National
595 Laboratory, Oak Ridge, Tennessee. 67 pp. doi: 10.3334/CDIAC/atg.ndp057

596 Pont, D., Simonnet, J.P., Walter, A.V. (2002) Medium-term changes in suspended
597 sediment delivery to the ocean: Consequences of catchment heterogeneity and
598 river management (Rhone River, France). Estuarine Coastal Shelf Sci. 54 (1), 1-
599 18.

600 Radakovitch O., Charmasson S., Arnaud M. and Bouisset P. (1999) ^{210}Pb and
601 caesium accumulation in the Rhône delta sediment. Estuarine Coastal Shelf Sci.
602 48, 77-99.

603 Reynolds, R.A., Stramski, D., Wright, V.M., Wozniak, S.B. (2010) Measurements and
604 characterisation of particle size distributions in coastal waters. J. Geophys. Res.
605 115, C08024, doi: 10.1029/2009JC005930.

606 Roussel-Debet, S. (2012) Constat radiologique Vallée du Rhône. Rapport final relatif
607 au milieu terrestre. Rapport IRSN PRP-ENV/SESURE/2012-06.

608 Roussiez V., Aloisi J. C., Monaco A. and Ludwig W. (2005) Early muddy deposits
609 along the Gulf of Lions shoreline: a key for a better understanding of land-to-sea
610 transfer of sediments and associated pollutant fluxes. Mar. Geol. 222, 345–358.

611 Trundinger C.M., Enting I.G., Francey R.J., Etheridge D.M., Rayner P.J. (1999)
612 Long-term variability in the global carbon cycle inferred from a high-precision
613 CO_2 and $\delta^{13}C$ ice-core record. Tellus B 51, 233–248.

Figure captions

Figure 1: Location of main nuclear activities in the Rhône catchment: power stations (in red) operated by Electricité de France (EDF) and nuclear facilities (in blue) operated by the French Atomic Energy Commission (CEA) and the AREVA company. Inset: location of the KBROUS and KB-06 cores taken in November 2001.

Figure 2: Tritium (HTO) airborne releases (Jean-Baptiste et al., 2018). Dotted curve: Marcoule releases. Solid curve: cumulative releases from Marcoule and Valduc.

Figure 3: Tritium liquid releases (Jean-Baptiste et al., 2018). Dotted curve: Marcoule releases. Solid black curve: cumulative releases from Marcoule and EDF nuclear power stations. Blue curve: cumulative releases from Marcoule, EDF nuclear power stations and indirect inputs to the Rhône by the contamination of the hydrographic network by tritium airborne releases (see Section 3.3.3).

Figure 4: Spatial distribution of the tritium (OBT) content of sediments along the Rhône in 2004-2005 (Gontier & Siclet, 2011).

Figure 5: Profiles of organically bound tritium (OBT) (in black) and carbon-14 (in blue) in the organic matter of (a) the KB-06 and (b) the KBROUS sediment core samples collected in 2001 at the mouth of the Rhône.

Figure 6: Comparison between the history of ^{239,240}Pu discharges from the Marcoule site (Eyrolle et al., 2004) and the vertical distribution of ^{239,240}Pu in the KBROUS core (Lansard et al., 2007) for a constant sedimentation rate of 0.186 m.yr^{-1}.

Figure 7: Correlation between ^{239,240}Pu and ^{241}Am (in Bq.kg^{-1} of dry sediment) for the KBROUS core (^{241}Am data are from the Institute of Radioprotection and Nuclear Safety - IRSN).

637 Figure 8: Comparison between the history of ^{241}Am discharges from the Marcoule
638 site and the vertical distribution of ^{241}Am in the KB-06 core for a constant
639 sedimentation rate of 0.025 $m.yr^{-1}$ (^{241}Am data are from IRSN).

640 Figure 9: Time-evolution of the tritium content of the organic matter (OBT) in the
641 KBROUS (solid black curve) and KB-06 (dotted black curve) cores. Red rectangle:
642 OBT in a surface sediment (0-3 cm) from the mouth of the Rhône in 1986-1987 by
643 Gontier et al., 1992; Red crosses: tritium content of suspended matter at Arles in
644 2010-2011 (Jean-Baptiste et al., 2018).

645 Figure 10: Organically bound tritium (OBT) for land vegetation in the environment
646 around Marcoule with the distance to the source of tritium discharges into the
647 atmosphere (Roussel-Debet, 2012). The black curve represents the exponential
648 decrease proposed by Baglan et al. (2011) to explain the data around the CEA site of
649 Bruyère-le-Châtel. The red curve is the one adopted for this study (see Section 6.3).

650 **Table captions**

651 Table 1: Tritium, carbon-14 and $\delta^{13}C$ measurements in the KBROUS sediment core.
652 ^{241}Am and $^{239,240}Pu$ data (in $Bq.kg^{-1}$ of dry sediment) are from the IRSN database and
653 Lansard et al. (2007), respectively.

654

655 Table 2: Tritium, carbon-14 and $\delta^{13}C$ measurements in the KB-06 sediment core.
656 ^{241}Am data (in $Bq.kg^{-1}$ of dry sediment) are from the IRSN database.

657

Depth (cm)	^{14}C (pmC)			$\delta^{13}C$ (‰)	OBT (TU)			Year (18.6 cm.yr^{-1})	OBT (TU) decay-corrected			^{241}Am (Bq.kg^{-1})			$^{239,240}Pu$ (Bq.kg^{-1})		
0-10	76,65	±	0,25	-26,30	1093	±	118	2001,59	1855	±	200	<0,7			0,256	±	0,012
10-20	67,06	±	0,34	-26,27	640	±	90	2001,05	1120	±	157	0,58	±	0,25			
20-30	74,79	±	0,27	-26,29	2296	±	250	2000,52	4141	±	451	<0,8			0,356	±	0,016
30-40	82,37	±	0,30	-26,45	2565	±	329	1999,98	4769	±	612	<1,2					
40-50	75,08	±	0,24	-26,45	1400	±	147	1999,44	2682	±	282	<1,1			0,357	±	0,014
50-60	65,88	±	0,25	-25,82	2088	±	302	1998,90	4123	±	596	<0,7					
60-70	67,31	±	0,32	-26,44	1906	±	194	1998,37	3879	±	395	<1,0			0,308	±	0,015
70-80	69,33	±	0,25	-26,17	1797	±	211	1997,83	3771	±	443	0,64	±	0,22	0,393	±	0,013
80-90	79,93	±	0,25	-26,49	2469	±	279	1997,29	5340	±	603	1,16	±	0,27	0,770	±	0,025
90-100	81,37	±	0,29	-26,41	2428	±	338	1996,75	5413	±	753	1,04	±	0,26			
100-110	72,49	±	0,24	-26,35	2508	±	315	1996,21	5762	±	724	<1,1			0,841	±	0,023
110-120	68,97	±	0,23	-26,31	2299	±	395	1995,68	5445	±	936	<1,2					
120-130	83,40	±	0,57	-26,41	2435	±	294	1995,14	5944	±	718	1,04	±	0,26	1,247	±	0,035
130-140	76,45	±	0,25	-26,21	1829	±	254	1994,60	4601	±	639	0,54	±	0,26			
140-150	77,26	±	0,29	-26,13	2289	±	222	1994,06	5935	±	575	0,66	±	0,28	0,616	±	0,018
150-160	70,46	±	0,22	-26,07	1664	±	162	1993,53	4448	±	433	<1,2			0,340	±	0,012
160-170	91,53	±	0,42	-26,42	2727	±	258	1992,99	7512	±	710	1,27	±	0,27	1,665	±	0,047
170-180	79,95	±	0,25	-26,35	3136	±	362	1992,45	8904	±	1029	1,21	±	0,3	1,225	±	0,032
180-190	87,16	±	0,64	-27,31	3131	±	311	1991,91	9162	±	911	2,8	±	0,4	2,768	±	0,069
190-200	84,57	±	0,36	-26,51	3148	±	327	1991,38	9497	±	986	2,5	±	0,4	2,142	±	0,051
200-210	80,63	±	0,34	-25,96	3663	±	389	1990,84	11388	±	1208	4,7	±	0,5	3,895	±	0,097
210-220	73,60	±	0,32	-26,02	4164	±	749	1990,30	13342	±	2402	5,0	±	0,5			
220-230	77,23	±	0,27	-25,99	4298	±	519	1989,76	14195	±	1714	5,1	±	0,5	3,983	±	0,115
230-240	84,34	±	0,30	-26,07	8720	±	1191	1989,23	29684	±	4054	7,2	±	0,6			
240-250	76,53	±	0,42	-26,11	4589	±	506	1988,69	16101	±	1774	5,9	±	0,6	4,770	±	0,127
250-260	74,46	±	0,29	-26,34	6163	±	895	1988,15	22289	±	3236	5,7	±	0,5			
260-270	118,30	±	0,34	-26,08	5226	±	616	1987,61	19482	±	2295	7,3	±	0,6	5,631	±	0,248
270-280	95,35	±	0,34	-25,68	7708	±	851	1987,08	29615	±	3269	9,0	±	0,7			
280-290	60,43	±	0,25		6038	±	600	1986,54	23913	±	2377	9,4	±	0,7	5,974	±	0,258
290-300	67,62	±	0,22	-26,15	3856	±	426	1986,00	15741	±	1738	6,2	±	0,6	3,394	±	0,088
300-310	57,51	±	0,23	-26,09	2540	±	311	1985,46	10687	±	1308	1,22	±	0,3	1,090	±	0,056
310-320	77,04	±	0,28	-26,13	3877	±	385	1984,92	16813	±	1669	4,4	±	0,5	2,896	±	0,072
320-330	79,82	±	0,25	-26,79	2842	±	328	1984,39	12700	±	1466	4,5	±	0,5	3,071	±	0,140
330-340	69,29	±	0,26	-25,66	3112	±	352	1983,85	14338	±	1623	2,5	±	0,4			
340-350				-25,83	3721	±	447	1983,31	17668	±	2122	3,1	±	0,4	2,838	±	0,137
350-360	66,61	±	0,27	-25,86	3621	±	448	1982,77	17720	±	2191	2,6	±	0,4			
360-370	62,76	±	0,30	-25,89	3660	±	450	1982,24	18461	±	2270	2,7	±	0,4	3,696	±	0,177
370-380	63,08	±	0,22	-25,82	3598	±	440	1981,70	18708	±	2289	2,13	±	0,29			
380-390	64,27	±	0,22	-25,60	7524	±	848	1981,16	40318	±	4544	2,4	±	0,4	2,499	±	0,122
390-400	62,85	±	0,27	-25,71	2965	±	317	1980,62	16377	±	1751	3,1	±	0,4			
400-410	64,80	±	0,45	-25,92	4419	±	493	1980,09	25156	±	2807	2,55	±	0,32	1,504	±	0,082
410-420				-25,86	2909	±	329	1979,55	17067	±	1931	1,22	±	0,27			
420-430	49,09	±	0,19	-25,47	3311	±	340	1979,01	20027	±	2056	0,87	±	0,3	1,057	±	0,048
430-440	59,79	±	0,21	-25,69	2595	±	335	1978,47	16178	±	2087	<0,7					
440-450	59,95	±	0,23	-25,95	2099	±	250	1977,94	13483	±	1606	<1,3			1,067	±	0,050
450-460	58,60	±	0,34	-25,11	2465	±	337	1977,40	16324	±	2234	<1,4					
460-470	49,97	±	0,24	-25,96	2221	±	309	1976,86	15161	±	2109	<1,1			0,630	±	0,029
470-473					1888	±	272	1976,51	13145	±	1892	<1,1			0,550	±	0,026

Depth (cm)	^{14}C (pmC)			$\delta^{13}C$ (‰)	OBT (TU)			Year (2.5 cm.yr^{-1})	OBT (TU) decay-corrected			^{241}Am (Bq.kg^{-1})		
0-10	59,61	±	0,22	-26,33	1212	±	153	1999,86	2269	±	287			
10-20	61,76	±	0,25	-26,70	2020	±	279	1995,86	4734	±	653			
20-30	79,98	±	0,30	-26,32	1921	±	237	1991,86	5640	±	695	0,71	±	0,27
30-40	74,44	±	0,25	-26,58	4272	±	505	1987,86	15703	±	1857	3,70	±	0,40
40-50	77,70	±	0,26	-26,19	3583	±	485	1983,86	16497	±	2233	4,40	±	0,50
50-60	62,98	±	0,24	-26,32	3380	±	424	1979,86	19489	±	2446	1,69	±	0,21
60-70	53,77	±	0,24	-25,97	2201	±	288	1975,86	15897	±	2083	1,16	±	0,29
70-80	41,62	±	0,20	-25,82	397	±	58	1971,86	3592	±	522	0,68	±	0,16
80-90	36,65	±	0,20	-26,46	24	±	9	1967,86	276	±	102	0,52	±	0,23
90-100	41,14	±	0,19	-25,59	19	±	7	1963,86	262	±	102			
100-110	34,99	±	0,18	-25,11	-			1959,86	-					
110-120	39,60	±	0,19	-25,51	-			1955,86	-					

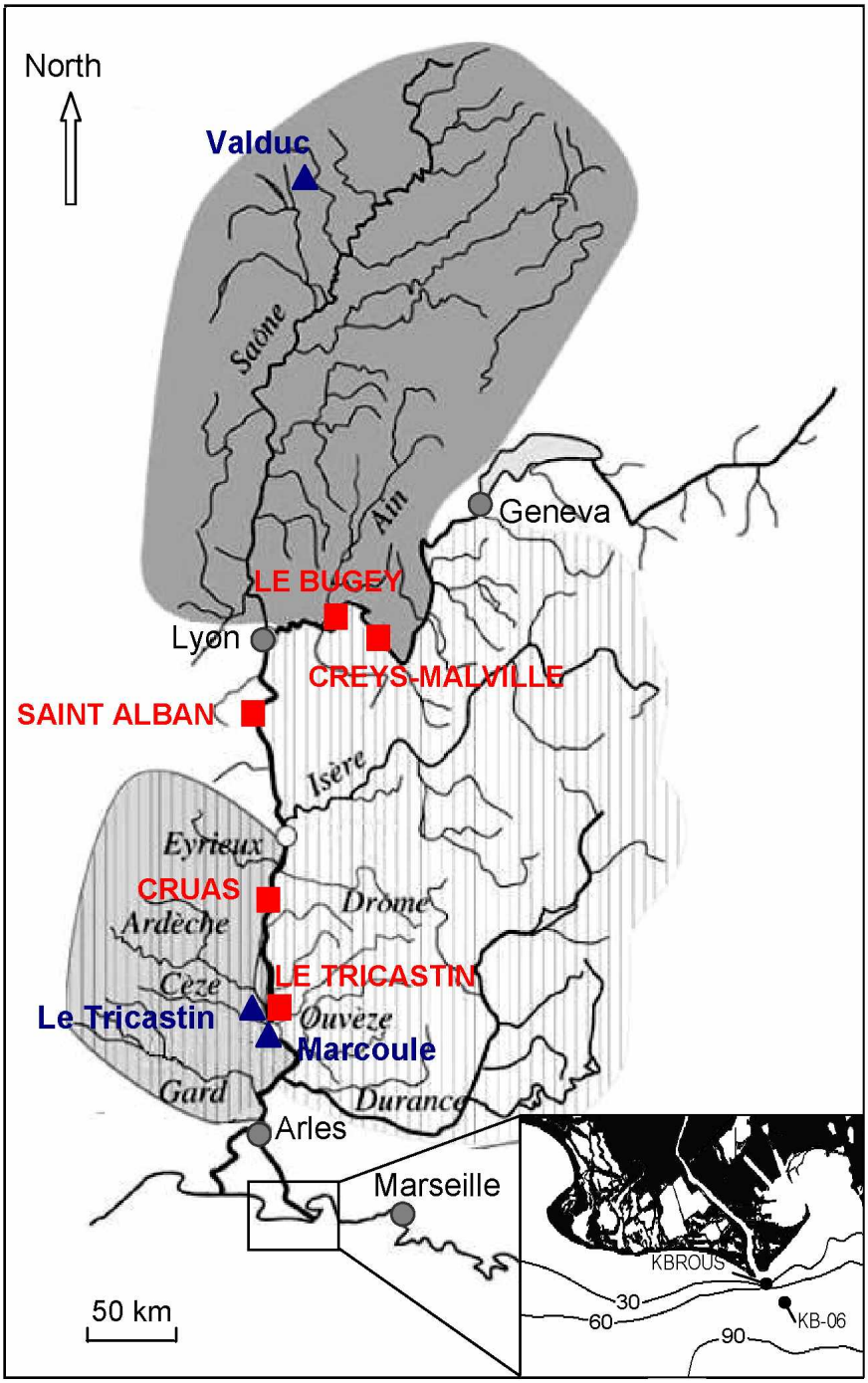
North
Valduc
Saône
Ain
Geneva
LE BUGEY
Lyon
CREYS-MALVILLE
SAINT ALBAN
Isère
Eyrieux
CRUAS
Drôme
Ardèche
Cèze
LE TRICASTIN
Le Tricastin
Ouvèze
Marcoule
Gard
Durance
Arles
Marseille
50 km
KBROUS
30
60
90
KB-06

Figure 1

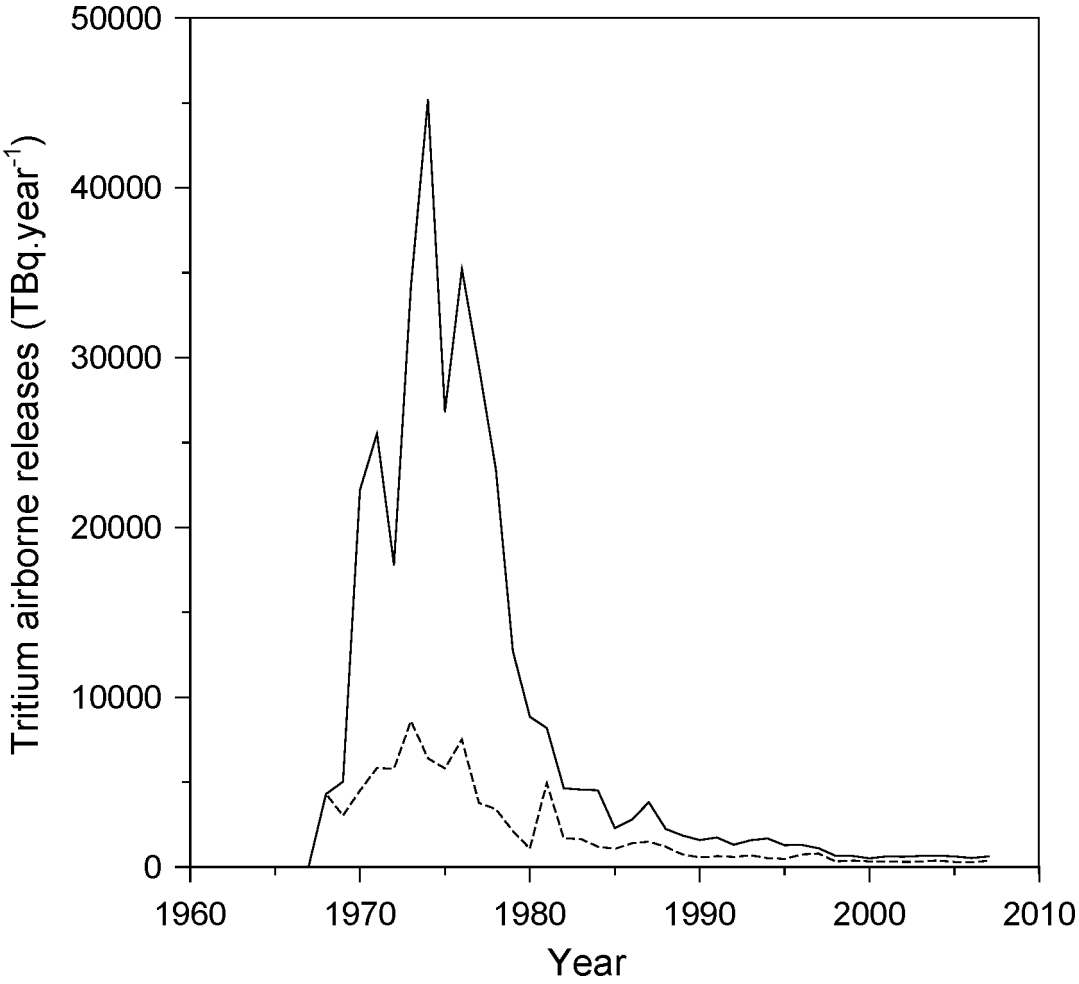
50000
40000
30000
20000
10000
0
Tritium airborne releases (TBq.year-1)
1960
1970
1980
1990
2000
2010
Year

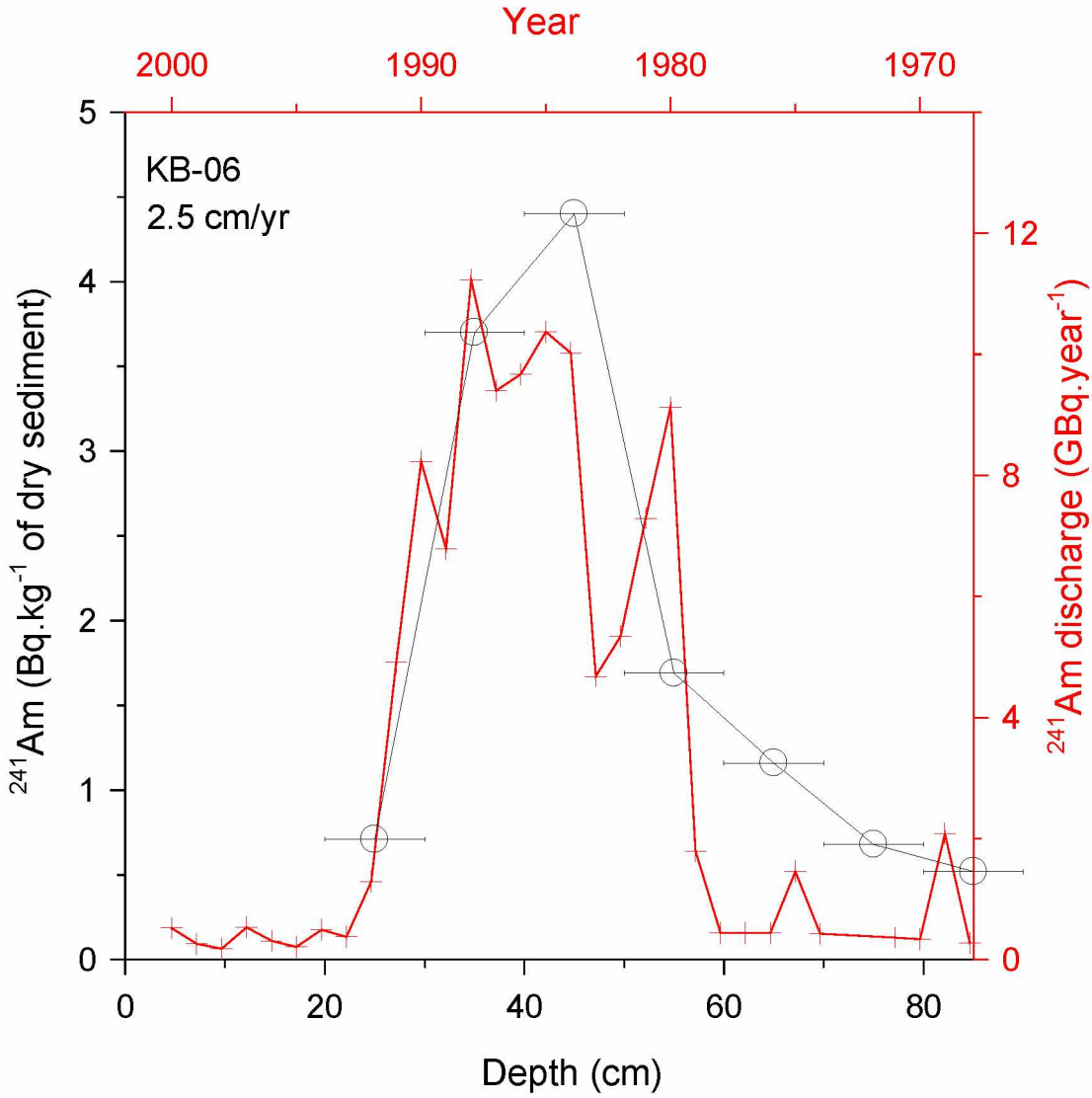
Year
2000
1990
1980
1970
KB-06
2.5 cm/yr
^{241}Am (Bq.kg^{-1} of dry sediment)
^{241}Am discharge (GBq.year^{-1})
Depth (cm)
0
1
2
3
4
5
0
4
8
12
0
20
40
60
80

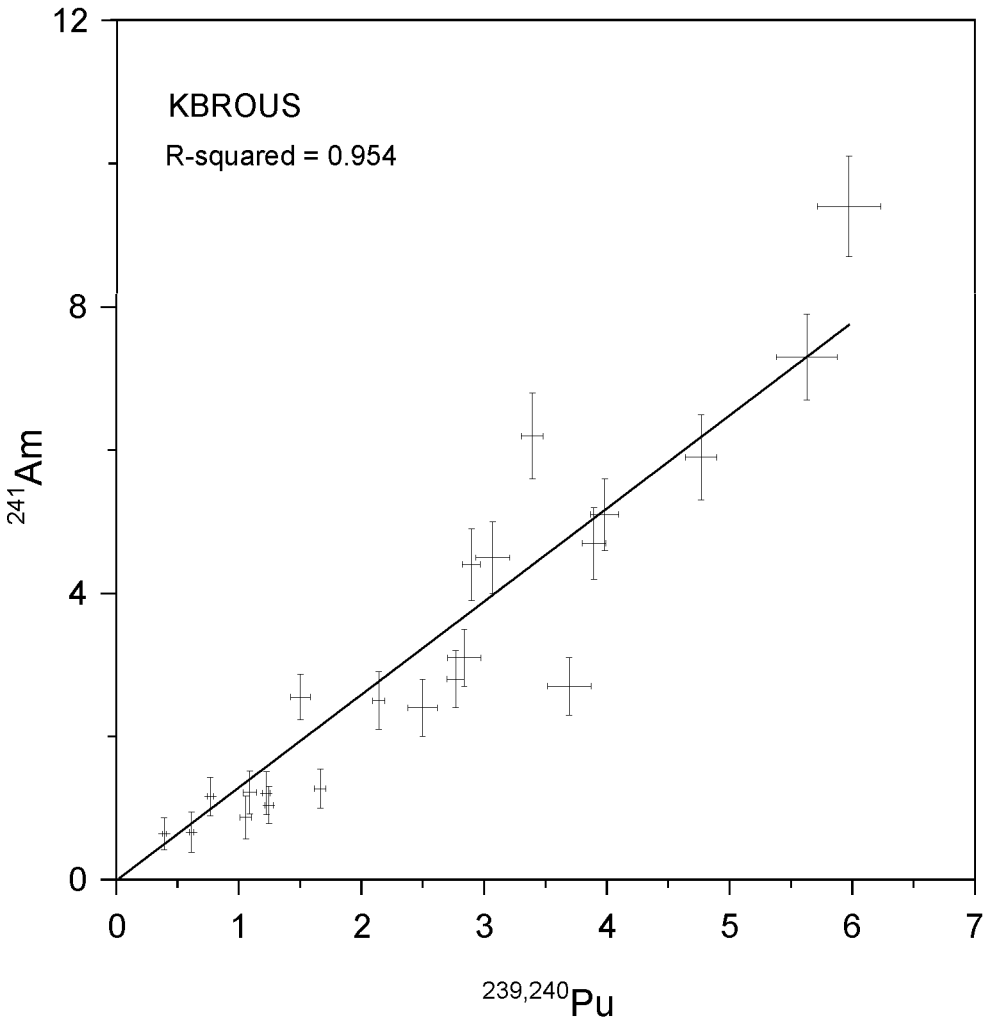
KBROUS
R-squared = 0.954
^{241}Am
^{239,240}Pu
0
4
8
12
0
1
2
3
4
5
6
7

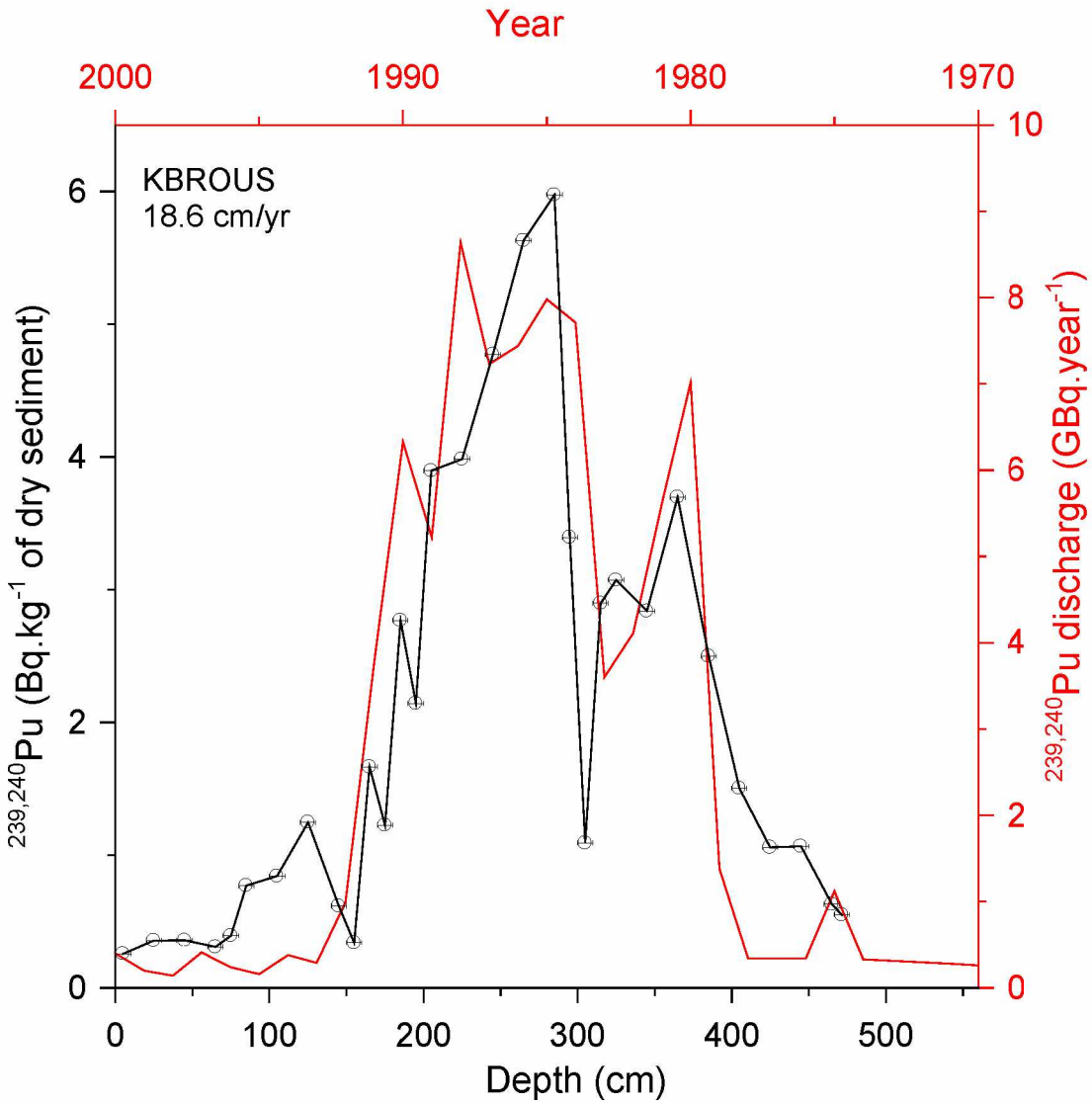
Year
2000
1990
1980
1970
KBROUS
18.6 cm/yr
239,240Pu (Bq.kg-1 of dry sediment)
239,240Pu discharge (GBq.year-1)
Depth (cm)
0
100
200
300
400
500
0
2
4
6
0
2
4
6
8
10

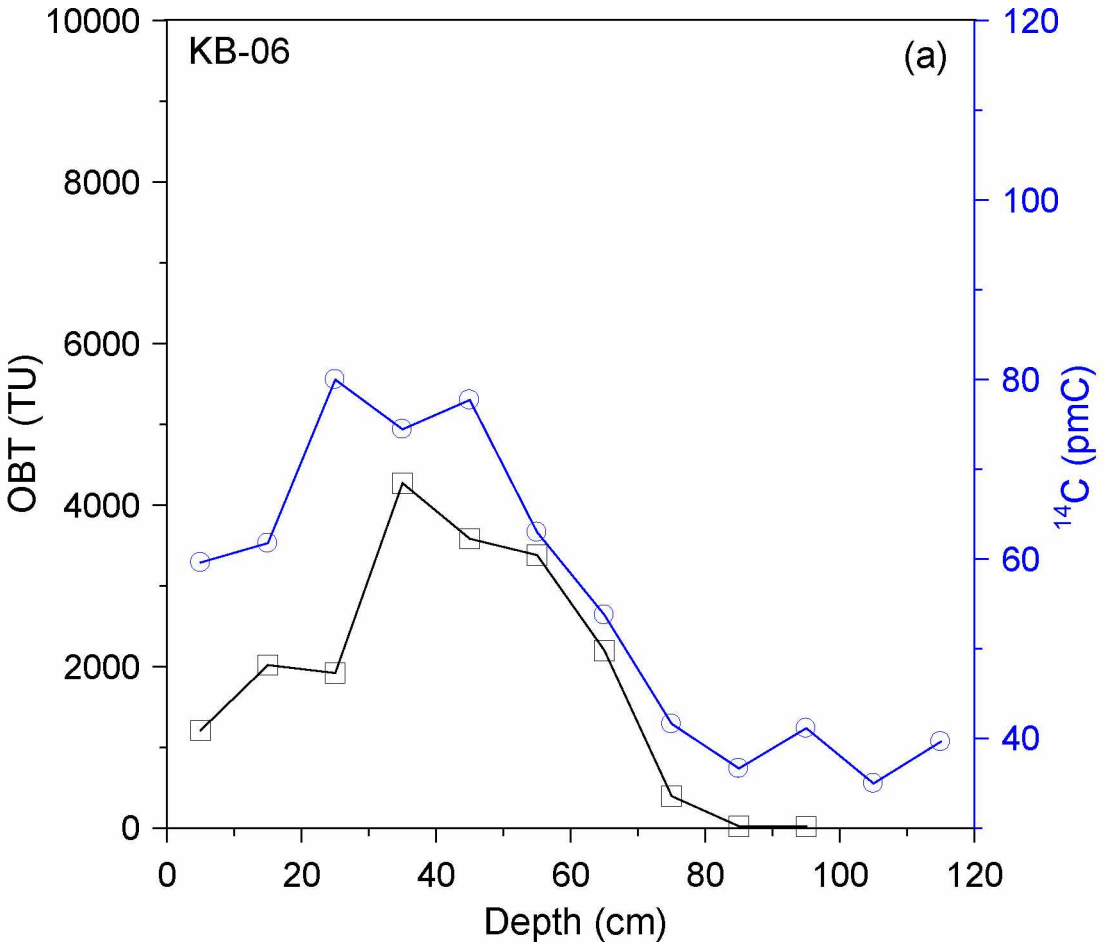
KB-06
(a)
OBT (TU)
^{14}C (pmC)
Depth (cm)
0
2000
4000
6000
8000
10000
40
60
80
100
120
0
20
40
60
80
100
120

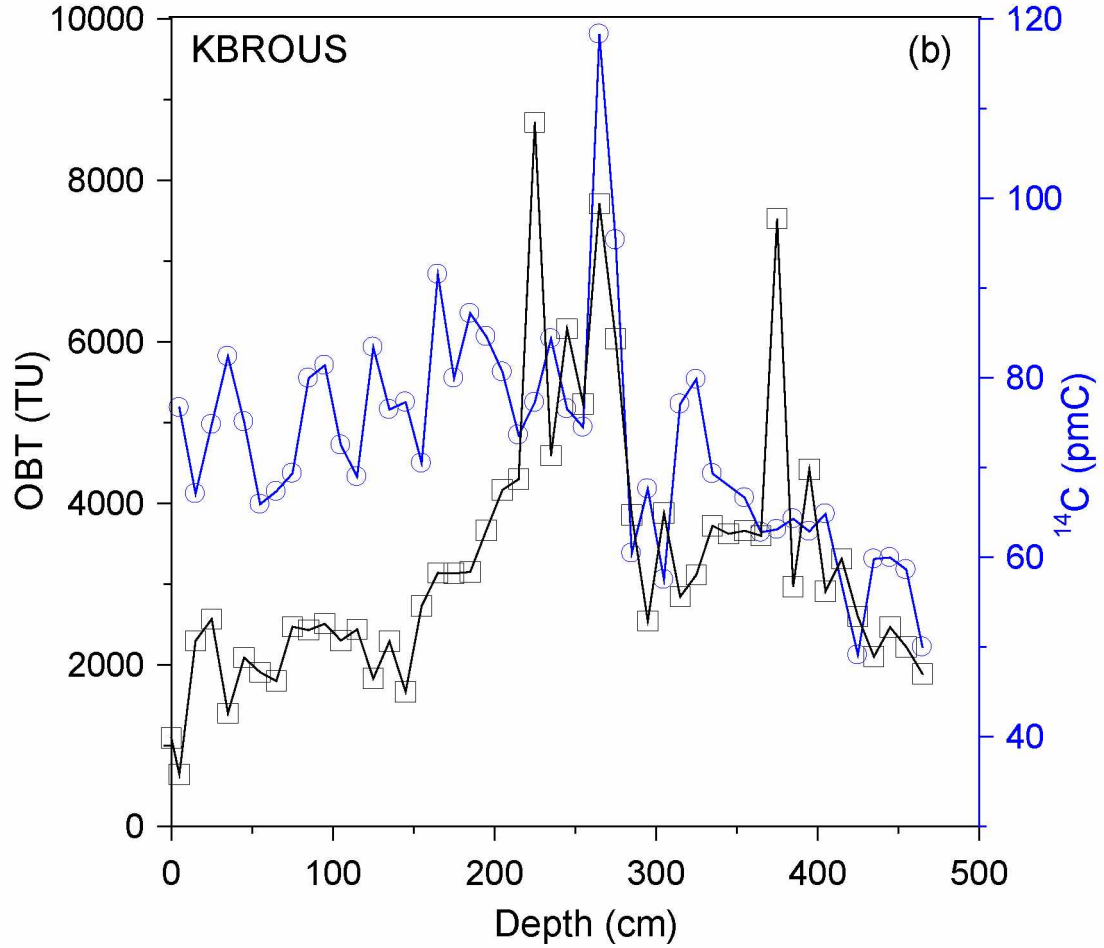
KBROUS
(b)
OBT (TU)
^{14}C (pmC)
Depth (cm)
0
2000
4000
6000
8000
10000
40
60
80
100
120
0
100
200
300
400
500

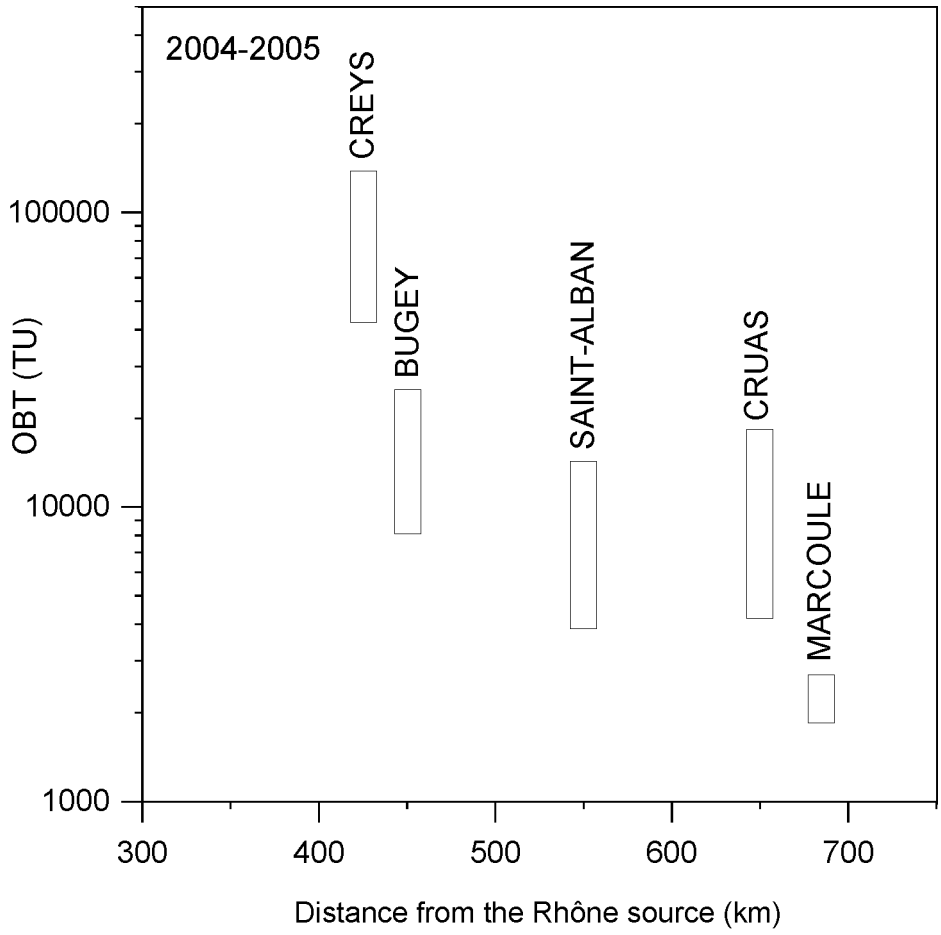
2004-2005
CREYS
BUGEY
SAINT-ALBAN
CRUAS
MARCOULE
OBT (TU)
100000
10000
1000
300
400
500
600
700
Distance from the Rhône source (km)

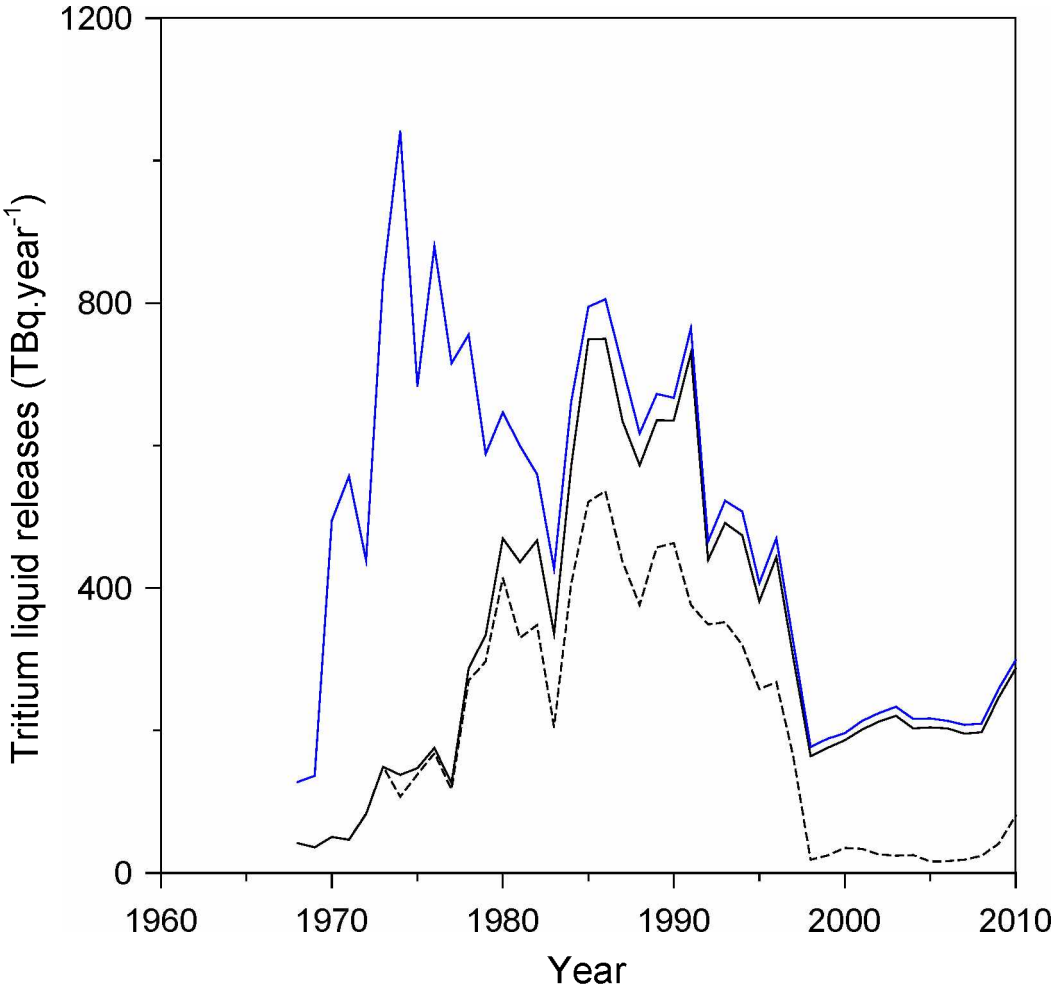
1200
800
400
0
Tritium liquid releases (TBq.year-1)
1960
1970
1980
1990
2000
2010
Year

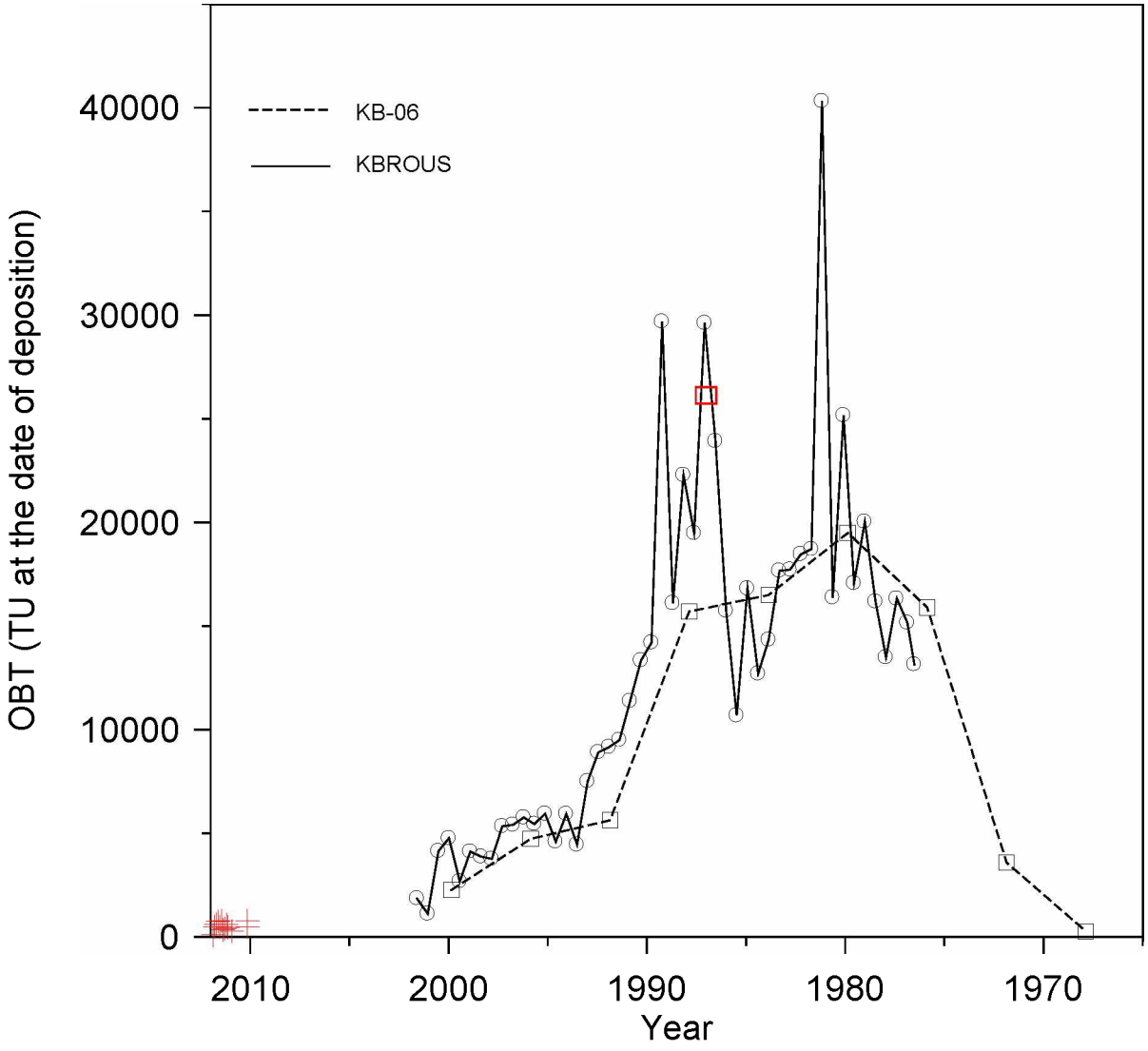
KB-06
KBROUS
OBT (TU at the date of deposition)
40000
30000
20000
10000
0
2010
2000
1990
1980
1970
Year

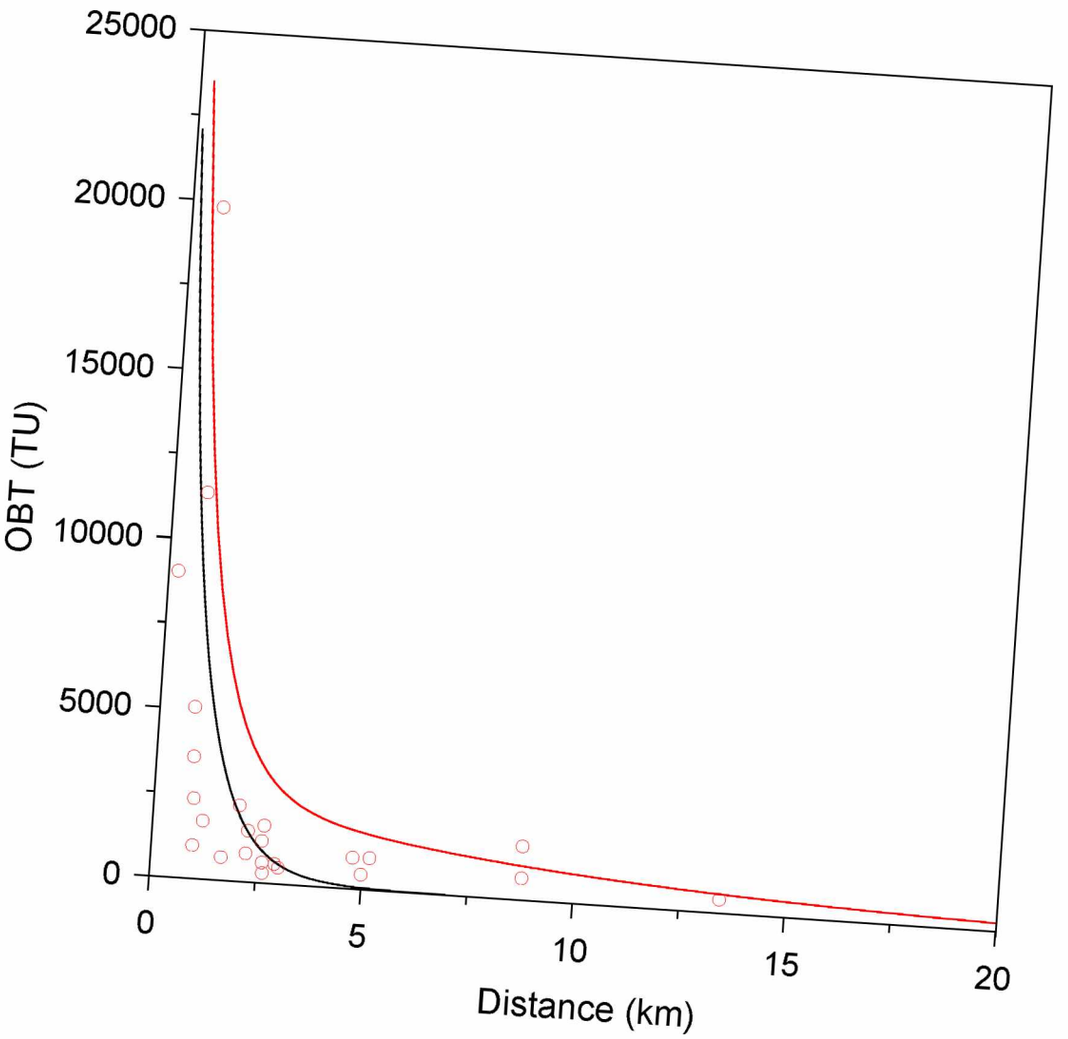
25000
20000
15000
10000
5000
0
OBT (TU)
0
5
10
15
20
Distance (km)